ACS APPLIED MATERIALS & INTERFACES

Research Article

www.acsami.org

Enhancing the Heat Transfer Efficiency in Graphene–Epoxy Nanocomposites Using a Magnesium Oxide–Graphene Hybrid Structure

Fei-peng Du,[†] Wen Yang,[†] Fang Zhang,[†] Chak-Yin Tang,*[,‡] Sheng-peng Liu,[†] Le Yin,[†] and Wing-Cheung Law[‡]

[†]School of Materials Science and Engineering and Key Laboratory of Green Chemical Process of Ministry of Education, Wuhan Institute of Technology, Wuhan 430073, China

[‡]Department of Industrial and Systems Engineering, The Hong Kong Polytechnic University, Hung Hom, Hong Kong, China

ABSTRACT: Composite materials, such as organic matrices doped with inorganic fillers, can generate new properties that exhibit multiple functionalities. In this paper, an epoxy-based nanocomposite that has a high thermal conductivity and a low electrical conductivity, which are required for the use of a material as electronic packaging and insulation, was prepared. The performance of the epoxy was improved by incorporating a magnesium oxide-coated graphene (MgO@GR) nanomaterial into the epoxy matrix. We found that the addition of a MgO coating not only improved the dispersion of the graphene in the matrix and the interfacial bonding between the graphene and epoxy but also enhanced the thermal conductivity of the epoxy while preserving the electrical insulation. By adding 7 wt % MgO@GR, the thermal conductivity of the epoxy nanocomposites was enhanced by 76% compared with that of the neat epoxy, and the electrical resistivity was maintained at 8.66×10^{14} Ω m.

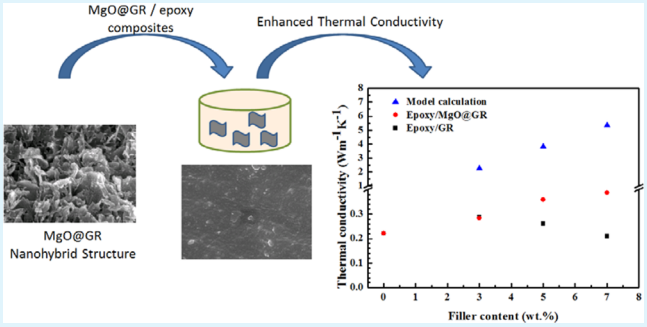

KEYWORDS: *epoxy, graphene, magnesium oxide, composites, thermal conductivity*

1. INTRODUCTION

Polymer-based materials (e.g., epoxy) are commonly used for electronic product packaging (e.g., electrical appliances and printed circuit boards) because of their excellent insulation properties.[1,2] Epoxy resins are attractive for use in electronic applications because they are compatible with a wide range of copolymerizations and adhesion, possess excellent corrosion resistance, and have a reasonable cost. However, one of the drawbacks in the use of epoxy resins is their low thermal conductivity. The inefficient removal of the heat generated when an electronic device is in operation may compromise the work stability and the lifetime of the device. Over the past two decades, composite materials have shown promising results in improving the thermal conductivity of polymers while retaining electrical insulation.[3−6] One of the most effective approaches has been to introduce inorganic micro- and nanofillers into the polymer matrix.[3] Specifically, graphene (GR) and carbon nanotubes (CNTs) exhibit extraordinary mechanical, electrical, and thermal characteristics that make them excellent fillers for improving the performance of composite materials. For example, the polymer modulus can be improved by several orders of magnitude (from gigapascals to terapascals) by filling the epoxy with CNTs or GRs.[7−9] These carbon nanomaterials appear to be ideal thermally conducting fillers in epoxy because of the ultrahigh thermal conductivity.[10−12] Several examples are multiwalled carbon nanotubes (~3000 W m^{-1} K^{-1}), single-walled carbon nanotubes (SWNTs) (~6000 W m^{-1} K^{-1}), and graphene (~5000 W m^{-1} K^{-1}). Data concerning the thermal properties have also been reviewed for carbon nanomaterials and their composites.[13] However, the reported thermal conductivities of carbon fillers/polymer nanocomposites are far lower than the required values.[14−16] The primary reason for this low thermal conductivity is the strong phonon scattering at the filler/polymer interface, which is due to the weak bonding and phonon modulus mismatch between the carbon nanofillers and the polymer matrix, which restricts the heat transfer along the nanocomposite.[7,15]

Some reports have shown that the interfacial interaction and the dispersion of fillers in the matrix can be improved by surface modifications of the carbon nanofillers with organic and inorganic layers.[17−20] Zhao et al. reported that coating silica on the CNT surfaces can substantially improve the phonon modulus mismatch between the polyurethane and CNTs.[21] Additionally, GR has been shown to have thermal conductive properties that are better than those of CNTs because of the two-dimensional lattice.[12,22−24] Teng et al. demonstrated that,

Received: April 13, 2015
Accepted: June 15, 2015
Published: June 15, 2015

DOI: 10.1021/acsami.5b03196
ACS Appl. Mater. Interfaces 2015, 7, 14397−14403

with the same filler concentration (4 phr), the thermal conductivity of a pyrene-modified GR/epoxy composite was 20% greater than that of an unmodified GR/epoxy composite and 267% greater than that of an unmodified CNT/epoxy composite. Recently, research efforts have been devoted to investigating the possibility of adding inorganic oxides [Al(OH)$_3$, Al_2O_3, ZnO, and TiO_2] as the interfacial layers to improve the thermal conductivity of the polymer matrix.[25−27] This research found that the interfacial interaction was improved by the hydrogen bonds that were developed from the hydroxyl groups (OH) created on the oxide surface of the filler.[28] The hydroxyl groups formed on the MgO surface generally resulted from the heterolytic dissociation of water molecules by two mechanisms (i.e., hydroxylation of surface cations and protonation of surface oxide ions). Among most of the commonly used inorganic oxides, magnesium oxide (MgO) possesses a high thermal conductivity value (~42 W m^{-1} K^{-1}) that is 32 times greater than the thermal conductivity of SiO_2.[29] In our previous study, MgO-coated multiwalled CNTs were used as filler to fabricate epoxy nanocomposites.[30] When the filling content reached 2.0 wt %, the thermal conductivity of the MgO-coated sample increased by 34% compared with that of the uncoated sample. Because of the superior properties of GR versus those of CNT, in this work, we attempted to further improve the thermal conductivity of epoxy by introducing MgO-coated GR into the epoxy resin (epoxy/MgO@GR). The surface morphologies and physical properties of the samples with various filler concentrations were characterized using field-emission scanning electron microscopy (FESEM), transmission electron microscopy (TEM), thermogravimetric analysis (TGA), and differential scanning calorimetry (DSC). Additionally, the thermal conductivity and electrical insulation of the nanocomposites were systematically measured to study the influence of the filler concentrations on the thermal properties of epoxy/MgO@GR.

2. EXPERIMENTAL SECTION

2.1. Materials. Raw graphite powder (120 μm) was supplied by Qingdao BCSM Co., Ltd. Diglycidyl ether of bisphenol A (DEBA) was obtained from Yueyang Petrochemical Co., Ltd. Curing agent 593 (diethylene triamine adduct with butyl glycidyl ether) was purchased from Hangzhou Wuhuigang Adhesive Co., Ltd. All other regents were analytical grade and were supplied by Sinopharm Chemical Reagent Co., Ltd.

2.2. Preparation of Graphite Oxide. Graphite oxide (GO) was prepared from natural graphite powder using the modified Hummers method. The typical procedure was as follows.[31,32] First, 1 g of graphite powder was dissolved in 23 mL of concentrated sulfuric acid in an ice bath (at 0 °C) while the sample was being stirred, and 3 g of $KMnO_4$ was then added slowly to the solution; the reaction mixture was kept in the ice bath for 1 h. Subsequently, the reaction mixture was held at 15 °C for 2 h followed by 35 °C for 30 min. Then, 80 mL of water was added to the reaction solution, and the mixture was maintained at 98 °C for 15 min. Finally, 20 mL of H_2O_2 (30 wt %) was added to remove the excess MnO_2. The sample during the entire procedure was subjected to continuous stirring. GO was obtained after the reaction solution had been filtered.

2.3. Synthesis of Magnesium Oxide-Coated Graphene (MgO@GR). The typical procedure was as follows.[30] First, 0.1 g of GO was dispersed in 100 mL of deionized water under ultrasonic processing for 1 h to obtain a homogeneous solution. Subsequently, 2 g of $MgCl_2{\cdot}6H_2O$ was added to the GO solution to provide Mg^{2+}, followed by the sample being stirred at 80 °C for 4 h. Next, 100 mL of a NaOH solution (0.2 mol/L) was added dropwise to the solution over the course of 30 min, and the stirring continued for 12 h for the formation of magnesium hydroxide. After vacuum filtration, the obtained solid was redispersed in 100 mL of deionized water under ultrasonic processing for 1 h, 1 g of $NaBH_4$ was then added, and the reaction occurred at 80 °C for 6 h to reduce the GO. The resulting mixture was vacuum-filtered and washed with alcohol and deionized water. Finally, magnesium oxide-coated graphene (MgO@GR) was obtained via calcining the collected powders at 600 °C under Ar protection for 2 h.

2.4. Preparation of Epoxy/MgO@GR Nanocomposites (epoxy/MgO@GR). MgO@GR (0.12 g) was dispersed in 2 mL of acetone under ultrasonic treatment for 30 min. After the temperature had been increased to 80 °C, 10 g of epoxy and 2 g of curing agent were added while the sample was being vigorously stirred for 1 h. Finally, via the casting method, the mixture was poured into a homemade mold, the air bubbles were removed at room temperature in a vacuum oven for 1 h, and the cast was cured at room temperature under atmospheric pressure for 24 h. Disclike specimens with a 100 mm diameter and 2 mm thickness were prepared. With reference to our previous research,[7,21] epoxy/MgO@GR nanocomposites with 3, 5, and 7 wt % MgO@GR were prepared by adjusting the weight ratio of MgO@GR and epoxy. Similar procedures were performed to prepare the epoxy/GR nanocomposites.

2.5. Characterization. The morphology of MgO@GR was observed using field-emission scanning electron microscopy (FESEM) (JEOL, JSM-6700F) and transmission electron microscopy (TEM) (FEI Co., Tecnai G220). Thermogravimetric analysis (TGA) measurements were performed in an air atmosphere using a heating rate of 10 °C/min provided by a TA Instruments Q50 thermal gravimetric analyzer, and the measurements were conducted using 6−10 mg samples. The DSC measurement of the thermal transition temperatures was performed on a TA Instruments Q20 differential scanning calorimeter equipped with a thermal analysis data station that was operating at a scanning rate of 10 °C/min in a nitrogen atmosphere. The thermal history of the samples was eliminated by heating them to 180 °C, holding for them at that temperature for 5 min, and then cooling the samples to 25 °C at a scan rate of 10 °C/min. The volumetric electrical resistivity and the thermal conductivity were tested at room temperature using our previously reported methods.[7,21] Disclike specimens with a diameter of 100 mm and a thickness of 2 mm were used to test the volumetric electrical resistivity using a a PC40B digital insulation resistance tester (Shanghai AB Electronics Co.) according to model GB/T 1410-2006, and the thermal conductivity was tested with a steady-state thermal conductivity meter (TC-II, Shanghai Fudan Tianxin Co., Ltd.) according to ASTM C518-02. Before testing, the two sides of disclike specimens were flattened to decrease the contact resistance.

3. RESULTS AND DISCUSSION

The overall thermal conductivity of a nanocomposite material relies on the content of the nanofillers in the polymer matrix. A monolayer or a few layers of graphene in the polymer matrix led to outstanding physical and thermal properties. Indeed, the surface functionalization of graphene via chemical reduction is an effective approach for obtaining better dispersion of the graphene in the nanocomposites. As reported in our previous research,[31,32] an abundance of carboxylic acid groups (-COOH groups) existed in the structure of GO. Before MgO@GR was obtained, magnesium cations (Mg^{2+}, from $MgCl_2$) were first chelated with carboxylic acid groups, and magnesium hydroxide then formed on the surface of the graphene oxide via the reaction of Mg^{2+} with the hydroxyl groups in an alkaline solution (by addition of NaOH). Subsequently, the magnesium hydroxide layer was transferred to the MgO layer after calcination. As the crystal behavior of GR is altered by covering it with an additional MgO layer, X-ray diffraction (XRD) can be used as an indirect approach to confirm the presence of MgO. XRD measurements in the 2θ range of 10−80° were conducted. As shown in Figure 1a, the XRD pattern of GR

DOI: 10.1021/acsami.5b03196
ACS Appl. Mater. Interfaces 2015, 7, 14397−14403

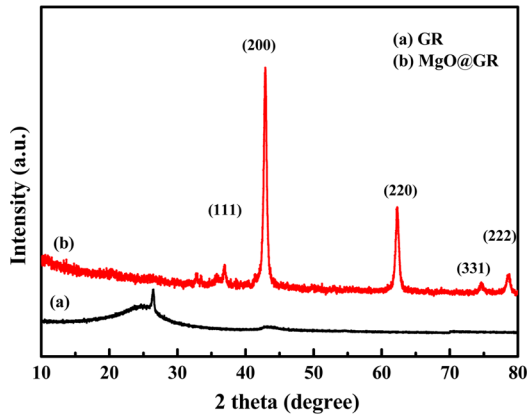

Figure 1. X-ray diffraction patterns of (a) GR and (b) MgO@GR.

was similar to our previously published data.[32] The two weak peaks at 25.3° and 26.4° confirm the existence of an individual graphene sheet with a stacking structure. After the reduction process and MgO coating, the diffuse distribution of the graphene diffraction peaks from 20° to 30° confirms the formation of GR hybrids (Figure 1b), which agrees with the observations described previously.[17,31,32] The diffraction peaks of the hybrid at 37.2°, 43°, 62.5°, 75°, and 78.8° correspond to lattice planes (111), (200), (220), (331), and (222), respectively, and indicate a standard pattern of the pure cubic phase of MgO with a crystalline lattice parameter *a* of 4.22 Å. These results show good agreement with the JCPDS data (75-0447),[33] which implies that the MgO@GR hybrids were successfully synthesized.

Figure 2a shows the "folding" structure of the untreated GR, which exhibits a smooth thin sheet surface without any additives or impurities. Following the MgO coating as shown in Figure 2b, some nanoparticles were found at the edges of the smooth surface and of thicker layers, which indicates the formation of MgO. Furthermore, the TEM image of GR clearly shows a transparent thin sheet with a wrinkled structure (Figure 2c). In contrast, the TEM image of MgO@GR shows that the nanoparticles or the inorganic layer was coated onto the surfaces of the GR sheets (Figure 2d). The thickness of the MgO layer can be estimated to be 10−20 nm when comparing the thickness with that of pure GR. The size of the MgO@GR sheets is approximately 400−800 nm, as shown in Figure 2d. The analysis of the XRD patterns and the SEM and TEM images indicates that nano-MgO was successfully coated onto the surface of the GR. As reported in other studies, the MgO can serve as a filler or an effective interface to facilitate the transfer of heat between the filler and the polymer matrix.[29,30]

To analyze the amount of loaded MgO, a TGA analysis of the MgO@GR hybrids was conducted. As shown in Figure 3a, there is approximately no mass loss below 100 °C in the GR sample and only 10 wt % mass loss in the GR sample when the temperature was between 100 and 400 °C, which implies that GR has good thermal stability at low temperatures. This mass loss is due to the decomposition of the oxygen-containing groups on the edge of the GR. When the temperature was >400 °C, the primary thermal decomposition began, and ∼86% of mass loss occurred between 400 and 520 °C, which was attributed to the decomposition of the carbon skeleton. When subjected to this high-temperature treatment, the sample subsequently vanished in the form of CO_2 gas without leaving any solid residue. For the MgO@GR sample, only 5 wt % of the mass was lost below 100 °C, which is attributed to absorbed water. Almost no mass loss occurs between 100 and 480 °C. The decomposition of the carbon−carbon skeleton occurred

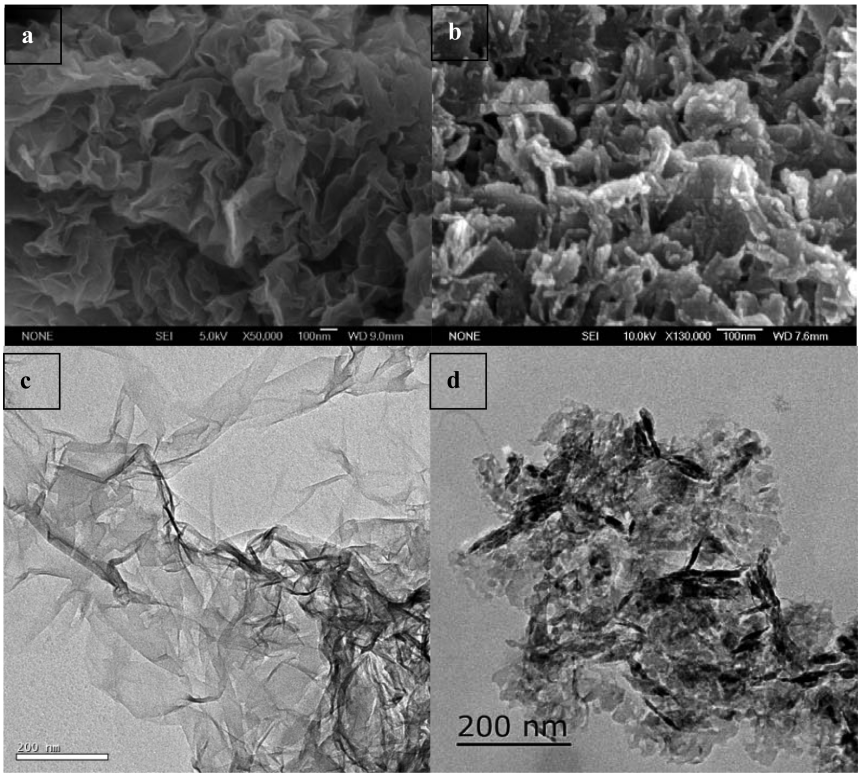

Figure 2. SEM images of (a) GR and (b) MgO@GR. TEM images of (c) GR and (d) MgO@GR.

DOI: 10.1021/acsami.5b03196
ACS Appl. Mater. Interfaces 2015, 7, 14397−14403

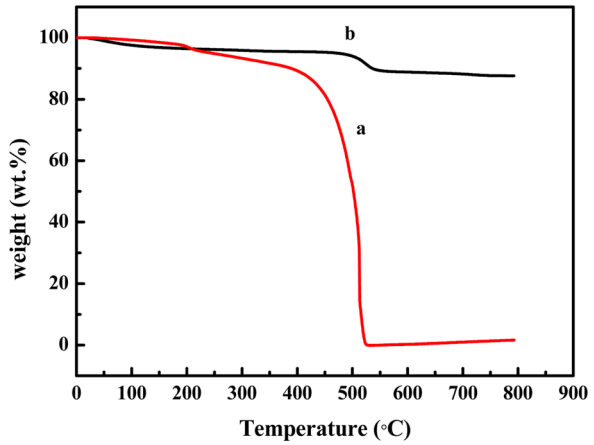

Figure 3. TGA curves of (a) GR and (b) MgO@GR in an air atmosphere.

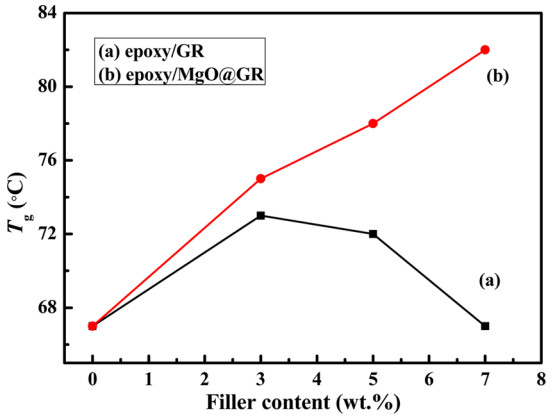

Figure 5. Relationship between T_g of the epoxy nanocomposites and the filler content.

between 480 and 540 °C. This result indicates that the addition of the MgO layer can enhance the thermal stability of the carbon skeleton in MgO@GRs and can protect the skeleton from decomposition at a high temperature.[34] At temperatures greater than 540 °C, the solid residues were MgO, and the amount of MgO in the MgO@GR hybrids was approximately 87.7 wt %, which was directly observed from the mass fraction of the residues, based on the TGA curve of the MgO@GR.

Good dispersion of the fillers in the polymer matrix is an important factor for achieving the desired performance. The dispersion of MgO@GR in the epoxy matrix was examined using SEM. Images of the cross section of the epoxy nanocomposites bulk are shown in Figure 4. Figure 4a shows the dispersion of GR in the epoxy matrix. Nonuniform distributions and a certain degree of agglomeration were observed. Moreover, microcracks are also observed in Figure 4a, which may result in a fragile fracture behavior that will affect the mechanical strength. For the MgO@GR-filled epoxy, the fillers are uniformly dispersed with a small size distribution. The enhanced dispersion can be attributed to the hydroxyl groups on the MgO surface. Similar to other inorganic particles, such as silica and alumina, the MgO interacted strongly with the epoxy groups.[7,27,35] Therefore, when MgO@GR is filled in an epoxy, a strong interfacial adhesion is formed because of the strong interaction of the MgO layer with the epoxy matrix.

DSC can indicate the interaction between the polymer matrix and the fillers by measuring the glass transition temperature (T_g). Figure 5 shows the relationship between the T_g of the epoxy nanocomposites and the filler content. The T_g value of the neat epoxy was ~67 °C, as shown in Figure 5. For the epoxy/GR nanocomposites (curve a), the T_g increased by 5 °C (73 °C) after 3 wt % GR had been added to the epoxy. However, upon addition of more GR, the T_g values decreased, i.e., ~72 °C for 5 wt % GR and ~67 °C for 7 wt % GR. For the epoxy/MgO@GR nanocomposites (curve b), the T_g of the neat epoxy increased from 67 °C (neat) to 75, 78, and 82 °C for 3, 5, and 7 wt % MgO@GR loading, respectively.

The increase in T_g can be attributed to the restriction of the molecular motion, a decrease in the free volume, and a greater degree of cross-linking in the polymeric system.[7] The reduction in T_g for the epoxy/GR nanocomposites suggests that the interaction between the GR and the epoxy molecular chain is weak because of the inert surface of graphene. With the increase in GR loading content, serious aggregation of GR occurred and further weakened the interaction of the GR and the epoxy matrix, which decreased T_g. Compared with that of the epoxy/GR nanocomposites, the epoxy/MgO@GR nanocomposites have a greater T_g value at the same filler content, which suggests that MgO@GR more strongly interacts with the epoxy because of the MgO coupling layer. Therefore, a stronger adhesive interface was created to restrict the mobility of the polymer chain. Because of the uniform dispersion of MgO@GR in the epoxy matrix (i.e., less aggregation), a greater loading content of MgO@GR resulted in a stronger restriction and, hence, a greater T_g value.

The thermal conductivities of the neat epoxy, the epoxy/GR and epoxy/MgO@GR nanocomposites at room temperature are shown in Figure 6. The thermal conductivity of the neat epoxy was 0.2210 W m^{-1} K^{-1} and increased with an increased MgO@GR content. It is worth noting that a high thermal conductivity was obtained (0.3819 W m^{-1} K^{-1}) with 7 wt %

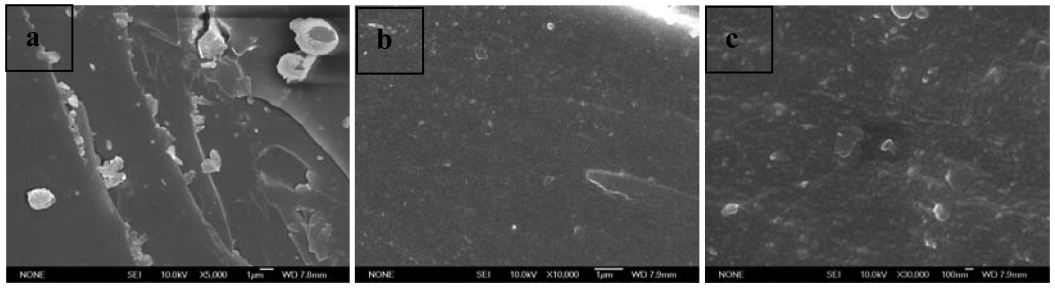

Figure 4. SEM micrographs of the epoxy nanocomposites loaded with (a) 5 wt % GR and (b) 5 wt % MgO@GR, and (c) magnified SEM micrographs of MgO@GR.

DOI: 10.1021/acsami.5b03196
ACS Appl. Mater. Interfaces 2015, 7, 14397−14403

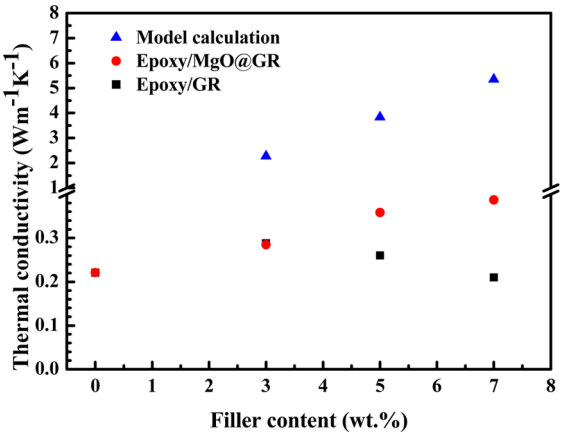

Figure 6. Experimental and calculated thermal conductivity of the epoxy nanocomposites.

MgO@GR, which corresponds to a 76% increase compared to the value for the neat the epoxy. However, the improvement obtained from the GR without the MgO coating was not obvious; i.e., the values increased by 30.4% (0.2883 W m^{-1} K^{-1}) and 17.7% (0.2600 W m^{-1} K^{-1}) and decreased by 5% (0.2100 W m^{-1} K^{-1}) when 3, 5, and 7 wt % GR was loaded into the neat epoxy, respectively.

As shown in Figure 6, the use of GRs as fillers resulted in little improvement in the thermal conductivity. This is because, on one hand, the small active surface of the GR resulted in a weak adhesion with the epoxy matrix, which prohibits the propagation of the phonon in the weak interface. Conversely, the agglomeration of GR in the epoxy matrix blocks the effective heat transport along the nanocomposites. Moreover, the agglomeration produced serious phonon scattering among the contacts with the GR sheets, which is similar to reports in the case of carbon nanotubes.[14,36] Therefore, the thermal conductivity of the epoxy nanocomposites with 7 wt % GR is lower than the value for 3 wt % and even lower than that for the neat epoxy. As confirmed by the SEM images and the DSC data, the MgO layer on the surface of the GR sheets strengthens the dispersion of GR and the interfacial adhesion between the GR and epoxy matrix, which leads to reduced interfacial thermal resistance.

The thermal conductivities of the epoxy composites with various filler concentrations can be modeled using eq 1[37,38]

$$\frac{K_c}{K_m} = \frac{1 + f_{MgO}(K_{MgO}^{eff}/K_m)/3 + 2f_{GR}^{eff}(K_{GR}/K_m)/3}{1 - (2f_{MgO} + f_{GR})} \quad (1)$$

where K_c, K_m, K_{MgO}, and K_{GR} are the thermal conductivities of the composite, the matrix, the MgO, and the GR, respectively, and f_{MgO} and f_{GR} are the volume fractions of the MgO and GR, respectively. For the sake of simplicity, literature values were used: K_m of 0.2210 W m^{-1} K^{-1}, K_{MgO} of ~30 W m^{-1} K^{-1},[39] and K_{GR} of 1500 W m^{-1} K^{-1}.[13,38] The volume fraction of MgO and GR in the epoxy/MgO@GR nanocomposite can be estimated on the basis of the density and the weight fraction of the filler in the composites using eq 2.

$$f_{GR} = \left(W_{MgO@GR} \times 12.3\%/\rho_{GR}\right)/\left[W_{MgO@GR} \times 12.3\%/\rho_{GR} + W_{MgO@GR} \times 87.7\%/\rho_{MgO} + (100 - W_{MgO@GR})/\rho_m\right] \quad (2)$$

In our calculations, the volume fraction of GR (f_{GR}) was estimated using the experimental results, where the weight content of the GR in MgO@GR was 12.3 wt %, as seen in the TGA curve, and $W_{MgO@GR}$ is the actual weight of the MgO@GR hybrid. ρ_{GR}, ρ_{MgO}, and ρ_m are the densities of the GR (2.2 g/cm^3),[40] the MgO (3.58 g/cm^3),[39] and the epoxy resin (1.2 g/cm^3), respectively.

The calculated result is shown in Figure 6 (▲). When the filler content increases, the thermal conductivity of the composite increases. We note that our experimental results on the epoxy/MgO@GR nanocomposite agreed with this trend. In contrast, a decrease in the thermal conductivity was obtained with an increase in GR filler content, which could be attributed to the poor dispersity of GR in the epoxy matrix that led to agglomeration. Via comparison of the calculated value with the experimental data, differences in the absolute value of thermal conductivity due to the phonon scattering at the interface of MgO@GR and the epoxy exist. The increasing trend of the model (◆) indicates that the MgO layer can improve the dispersion and thermal conduction between the GR and the polymer matrix.

Table 1 provides a comparative overview of the thermal conductivity of the epoxy/MgO@GR composites with the reported polymer/modified GR composites.[25,27,38,41,42] In this study, the magnitude of the improvement achieved using MgO@GR was comparable to that resulting from other reported methods.[25,27,41] For example, when the GR was modified with 3 wt % $Al(OH)_3$, the thermal conductivity of the epoxy increased by 35%,[25] whereas for GR modified with 10 wt % Al_2O_3, the thermal conductivity of the PVDF matrix increased by 80%.[27] The thermal conductivity of the epoxy that contained 2 wt % amino-graphene was increased by 36%.[41] In this study, epoxy nanocomposites with 7 wt % MgO@GR contain only 12.3 wt % GR based on the TGA curves of MgO@GR. However, the thermal conductivities of the polymer/GR nanocomposites described above are lower than the calculated data and previous results. Balandin et al. reported

Table 1. Thermal Conductivity of Various Polymer/GR Composites

material	content of GR in GR hybrid (%)	filler loading	enhancement of thermal conductivity compared to that of the neat polymer (%)	ref
epoxy/$Al(OH)_3$@GR	–	3 wt %	35	25
PVDF/GR@Al_2O_3	5	10 wt %	80	27
epoxy/amine-GR	–	2 wt %	36	41
PI/glycidyl methacrylate-GR	>50	5 wt %	261	42
PVA/GR/Ag	–	1.0 vol %	153	38
epoxy/MgO@GR	12.3	7 wt %	76	this work

DOI: 10.1021/acsami.5b03196
ACS Appl. Mater. Interfaces 2015, 7, 14397−14403

that the oriented graphene flakes in the matrix and the strong binding with the hydrocarbon-based matrix contributed to the large enhancement of the thermal conductivity.[40,43,44] The use of MgO-modified GR is an effective strategy for improving the interfacial thermal resistance of polymer/GR nanocomposites. More importantly, the preparation procedures are relatively simple, and the raw materials used for the synthesis are more cost-effective in our study. Therefore, the oriented distribution of the GR hybrid in the matrix will be analyzed in our future work.

Figure 7 shows the volumetric electrical resistivity of the epoxy/GR nanocomposites and the epoxy/MgO@GR nanocomposites. The electrical resistivity of the neat epoxy was 2.12 × 10^{16} Ω m. At a high GR loading (7 wt %), the electrical resistivity decreased sharply by 5 orders of magnitude and reached 1.31 × 10^{11} Ω m, which indicates that the electrical percolating network had already formed through the epoxy matrix.

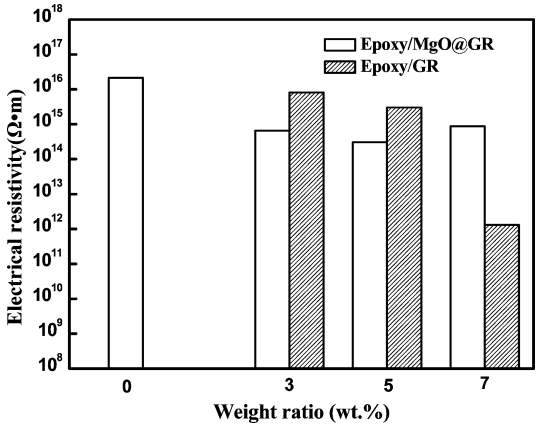

Figure 7. Volumetric electrical resistivity of the epoxy nanocomposites.

In sharp contrast, the volumetric electrical resistivity of the epoxy/MgO@GR nanocomposites was retained at a high electrical insulation value (8.66 × 10^{14} Ω m), even if the filler content was increased to 7 wt %. As reported, MgO is an inorganic filler with a large electrical insulation resistance and a high thermal conductivity.[39,45] The electrical insulation can increase the tunneling energy barrier and limit the inter-graphene charge transport in the polymer matrix, which is similar to the role of alumina or silica, as described in refs 7 and 27. Therefore, the high thermal conductivity of the MgO on the surface of the GR significantly reduced the thermal interfacial resistance of the nanocomposites while retaining excellent electrical insulation. This performance is superior to the use of silica as previously described.[7]

4. CONCLUSION

MgO@GR hybrids were successfully prepared by coating MgO onto the surface of graphene using a simple chemical precipitation method. MgO served as an effective interface. With better dispersion, the interfacial adhesion between the MgO@GR and the epoxy matrix was strengthened, which led to the improved thermal conductivity of the epoxy. When the epoxy nanocomposites were loaded with 7 wt % MgO@GR, which contained only 12.3 wt % GR, the thermal conductivity increased by 76%. Moreover, the electrical insulation of the MgO layer effectively inhibited the electron transport of the GR in the epoxy. The prepared epoxy nanocomposites exhibited both outstanding thermal conductivity and electrical insulation performance, which leads to good application prospects in the field of thermal management and electrical packaging.

AUTHOR INFORMATION

Corresponding Author

*E-mail: mfcytang@polyu.edu.hk.

Notes

The authors declare no competing financial interest.

ACKNOWLEDGMENTS

We acknowledge funding support from the Natural National Science Foundation of China (51373126), the Science Research Council of the Wuhan Institute of Technology (k201463), and the Opening Project of Key Laboratory of Green Chemical Process of Ministry of Education (GCP201207).

REFERENCES

(1) Li, T.; Zhang, J.; Wang, H.; Hu, Z.; Yu, Y. High-Performance Light-Emitting Diodes Encapsulated with Silica-Filled Epoxy Materials. *ACS Appl. Mater. Interfaces* **2013**, *5*, 8968−8981.

(2) Zhou, Y.; Yao, Y.; Chen, C. Y.; Moon, K.; Wang, H.; Wong, C. P. The Use of Polyimide-modified Aluminum Nitride Fillers in AlN@PI/Epoxy Composites with Enhanced Thermal Conductivity for Electronic Encapsulation. *Sci. Rep.* **2014**, *4*, 4779.

(3) Han, Z.; Fina, A. Thermal Conductivity of Carbon Nanotubes and Their Polymer Nanocomposites: A Review. *Prog. Polym. Sci.* **2011**, *36*, 914−944.

(4) Li, Y.; Huang, X.; Hu, Z.; Jiang, P.; Li, S.; Tanaka, T. Large Dielectric Constant and High Thermal Conductivity in Poly(vinylidene fluoride)/Barium Titanate/Silicon Carbide Three-Phase Nanocomposites. *ACS Appl. Mater. Interfaces* **2011**, *3*, 4396−4403.

(5) Jin, W.; Yuan, L.; Liang, G.; Gu, A. Multifunctional Cyclotriphosphazene/Hexagonal Boron Nitride Hybrids and Their Flame Retarding Bismaleimide Resins with High Thermal Conductivity and Thermal Stability. *ACS Appl. Mater. Interfaces* **2014**, *6*, 14931−14944.

(6) Balachander, N.; Seshadri, I.; Mehta, R. J.; Schadler, L. S.; Borca-Tasciuc, T.; Keblinski, P.; Ramanath, G. Nanowire-filled Polymer Composites with Ultrahigh Thermal Conductivity. *Appl. Phys. Lett.* **2013**, *102*, 093117.

(7) Cui, W.; Du, F.; Zhao, J.; Zhang, W.; Yang, Y.; Xie, X.; Mai, Y. Improving Thermal Conductivity while Retaining High Electrical Resistivity of Epoxy Composites by Incorporating Silica-coated Multi-walled Carbon Nanotubes. *Carbon* **2011**, *49*, 495−500.

(8) Yoonessi, M.; Lebrón-Colón, M.; Scheiman, D.; Meador, M. A. Carbon Nanotube Epoxy Nanocomposites: The Effects of Interfacial Modifications on the Dynamic Mechanical Properties of the Nanocomposites. *ACS Appl. Mater. Interfaces* **2014**, *6*, 16621−16630.

(9) Lee, C.; Wei, X.; Kysar, J. W.; Hone, J. Measurement of the Elastic Properties and Intrinsic Strength of Monolayer Graphene. *Science* **2008**, *321*, 385−388.

(10) Berber, S.; Kwon, Y. K.; Tománek, D. Unusually High Thermal Conductivity of Carbon Nanotubes. *Phys. Rev. Lett.* **2000**, *84*, 4613−4616.

(11) Kim, P.; Shi, L.; Majumdar, A.; McEuen, P. L. Thermal Transport Measurements of Individual Multiwalled Nanotubes. *Phys. Rev. Lett.* **2001**, *87*, 215502.

(12) Balandin, A. A.; Ghosh, S.; Bao, W.; Calizo, I.; Teweldebrhan, D.; Miao, F.; Lau, C. N. Superior Thermal Conductivity of Single-Layer Graphene. *Nano Lett.* **2008**, *8*, 902−907.

(13) Balandin, A. A. Thermal Properties of Graphene and Nanostructured Carbon Materials. *Nat. Mater.* **2011**, *10*, 569−581.

(14) Huxtable, S. T.; Cahill1, D. G.; Shenogin, S.; Xue, L.; Ozisik, R.; Barone, P.; Usrey, M.; Strano, M. S.; Siddons, G.; Shim, M.; Keblinski,

DOI: 10.1021/acsami.5b03196
ACS Appl. Mater. Interfaces 2015, 7, 14397−14403

P. Interfacial Heat Flow in Carbon Nanotube Suspensions. *Nat. Mater.* **2003**, *2*, 731−734.
(15) Hu, M.; Shenogin, S.; Keblinski, P. Molecular Dynamics Simulation of Interfacial Thermal Conductance between Silicon and Amorphous Polyethylene. *Appl. Phys. Lett.* **2007**, *91*, 241910.
(16) Liu, Y.; Kumar, S. Polymer/Carbon Nanotube Nano Composite Fibers: A Review. *ACS Appl. Mater. Interfaces* **2014**, *6*, 6069−6087.
(17) Teng, C.; Ma, C. M.; Lu, C. H.; Yang, S. Y.; Lee, S. H.; Hsiao, M. C.; Yen, M. Y.; Chiou, K. C.; Lee, T. M. Thermal Conductivity and Structure of Non-covalent Functionalized Graphene/Epoxy Composites. *Carbon* **2011**, *49*, 5107−5116.
(18) Song, S. H.; Park, K. H.; Kim, B. H.; Choi, Y. W.; Jun, G. H.; Lee, D. J.; Kong, B. S.; Paik, K. W.; Jeon, S. Enhanced Thermal Conductivity of Epoxy−Graphene Composites by Using Non-Oxidized Graphene Flakes with Non-Covalent Functionalization. *Adv. Mater. (Weinheim, Ger.)* **2013**, *25*, 732−737.
(19) Yang, S. Y.; Ma, C. C. M.; Teng, C. C.; Huang, Y. W.; Liao, S. H.; Huang, Y. L.; Tien, H. W.; Lee, T. M.; Chiou, K. C. Effect of Functionalized Carbon Nanotubes on the Thermal Conductivity of Epoxy Composites. *Carbon* **2010**, *48*, 592−603.
(20) Gulotty, R.; Castellino, M.; Jagdale, P.; Tagliaferro, A.; Balandin, A. A. Effects of Functionalization on Thermal Properties of Single-Wall and Multi-Wall Carbon Nanotube-Polymer Nanocomposites. *ACS Nano* **2013**, *7*, 5114−5121.
(21) Zhao, J.; Du, F.; Cui, W.; Zhu, P.; Zhou, X.; Xie, X. Effect of Silica Coating Thickness on the Thermal Conductivity of Polyurethane/SiO_2 Coated Multiwalled Carbon Nanotube Composites. *Composites, Part A* **2014**, *58*, 1−6.
(22) Malekpour, H.; Chang, K. H.; Chen, J. C.; Lu, C. Y.; Nika, D. L.; Novoselov, K. S.; Balandin, A. A. Thermal Conductivity of Graphene Laminate. *Nano Lett.* **2014**, *14*, 5155−5161.
(23) Goli, P.; Ning, H.; Li, X.; Lu, C. Y.; Novoselov, K. S.; Balandin, A. A. Thermal Properties of Graphene-Copper-Graphene Heterogeneous Films. *Nano Lett.* **2014**, *14*, 1497−1503.
(24) Yan, Z.; Liu, G.; Khan, J. M.; Balandin, A. A. Graphene Quilts for Thermal Management of High-Power GaN transistors. *Nat. Commun.* **2012**, *3*, 827.
(25) Kim, J.; Yim, B.; Kim, J.; Kim, J. The Effects of Functionalized Graphene Nanosheets on the Thermal and Mechanical Properties of Epoxy Composites for Anisotropic Conductive Adhesives (ACAs). *Microelectron. Reliab.* **2012**, *52*, 595−602.
(26) Choi, S.; Kim, K.; Nam, J.; Shim, S. E. Synthesis of Silica-coated Graphite by Enolization of Polyvinylpyrrolidone and Its Thermal and Electrical Conductivity in Polymer Composites. *Carbon* **2013**, *60*, 254−265.
(27) Qian, R.; Yu, J.; Wu, C.; Zhai, X.; Jiang, P. Alumina-coated Graphene Sheet Hybrids for Electrically Insulating Polymer Composites with High Thermal Conductivity. *RSC Adv.* **2013**, *3*, 17373−17379.
(28) Li, Y.; Sun, X. S. Preparation and Characterization of Polymer-Inorganic Nanocomposites by In Situ Melt Polycondensation of L-Lactic Acid and Surface-Hydroxylated MgO. *Biomacromolecules* **2010**, *11*, 1847−1855.
(29) Jeong, I. B.; Kim, J. S.; Lee, J. Y.; Hong, J. W.; Shin, J. Y. Electrical Insulation Properties of Nanocomposites with SiO_2 and MgO Filler. *Transactions on Electrical and Electronic Materials* **2010**, *11*, 261−265.
(30) Du, F.; Tang, H.; Huang, D. Y. Thermal Conductivity of Epoxy Resin Reinforced with Magnesium Oxide Coated Multiwalled Carbon Nanotubes. *Int. J. Polym. Sci.* **2013**, *2013*, 541823.
(31) Du, F.; Wang, J.; Tang, C. Y.; Tsui, C. P.; Xie, X. L.; Yung, K. F. Enhanced Electrochemical Capacitance of Polyaniline/Graphene Hybrid Nanosheets with Graphene as Templates. *Composites, Part B* **2013**, *53*, 376−381.
(32) Du, F.; Wang, J.; Tang, C. Y.; Tsui, C. P.; Zhou, X. P.; Xie, X. L.; Liao, Y. G. Water-Soluble Graphene Grafted by Poly(sodium 4-styrenesulfonate) for Enhancement of Electric Capacitance. *Nanotechnology* **2012**, *23*, 475704.
(33) Vu, A. T.; Jiang, S.; Kim, Y. H.; Lee, C. H. Controlling the Physical Properties of Magnesium Oxide Using a Calcination Method in Aerogel Synthesis: Its Application to Enhanced Sorption of a Sulfur Compound. *Ind. Eng. Chem. Res.* **2014**, *53*, 13228−13235.
(34) Zhu, H.; Yang, H.; Fu, W.; Zhu, P.; Li, M.; Li, Y.; Sui, Y.; Liu, S.; Zou, G. The Improvement of Thermal Stability of $BaMgAl_{10}O_{17}:Eu^{2+}$ coated with MgO. *Mater. Lett.* **2008**, *62*, 784−786.
(35) Chizallet, C.; Costentin, G.; Che, M.; Delbecq, F.; Sautet, P. Infrared Characterization of Hydroxyl Groups on MgO: A Periodic and Cluster Density Functional Theory Study. *J. Am. Chem. Soc.* **2007**, *129*, 6442−6452.
(36) Kim, P.; Shi, L.; Majumdar, A.; McEuen, P. L. Mesoscopic Thermal Transport and Energy Dissipation in Carbon Nanotubes. *Physica B* **2002**, *323*, 67−70.
(37) Chu, K.; Li, W. S.; Jia, C. C.; Tang, F. L. Thermal Conductivity of Composites with Hybrid Carbon Nanotubes and Graphene Nanoplatelets. *Appl. Phys. Lett.* **2012**, *101*, 211903.
(38) Li, Z.; Wang, D.; Zhang, M.; Zhao, L. Enhancement of the Thermal Conductivity of Polymer Composites with Ag−Graphene Hybrids as Fillers. *Phys. Status Solidi A* **2014**, *211*, 2142−2149.
(39) Slifka, A. J.; Filla, B. J.; Phelps, J. M. Thermal Conductivity of Magnesium Oxide from Absolute, Steady-State Measurements. *J. Res. Natl. Inst. Stand. Technol.* **1998**, *103*, 357−363.
(40) Goyal, V.; Balandin, A. A. Thermal Properties of the Hybrid Graphene-Metal Nano-Micro-Composites: Applications in Thermal Interface Materials. *Appl. Phys. Lett.* **2012**, *100*, 073113.
(41) Chatterjee, S.; Wang, J. W.; Kuo, W. S.; Tai, N. H.; Salzmann, C.; Li, W. L.; Hollertz, R.; Nüesch, F. A.; Chu, B. T. T. Mechanical Reinforcement and Thermal Conductivity in Expanded Graphene Nanoplatelets Reinforced Epoxy Composites. *Chem. Phys. Lett.* **2012**, *531*, 6−10.
(42) Tseng, I. H.; Chang, J. C.; Huang, S. L.; Tsai, M. H. Enhanced Thermal Conductivity and Dimensional Stability of Flexible Polyimide Nanocomposite Film by Addition of Functionalized Graphene Oxide. *Polym. Int.* **2013**, *62*, 827−835.
(43) Shahil, K. M. F.; Balandin, A. A. Graphene-Multilayer Graphene Nanocomposites as Highly Efficient Thermal Interface Materials. *Nano Lett.* **2012**, *12*, 861−867.
(44) Renteria, J. D.; Nika, D. L.; Balandin, A. A. Graphene Thermal Properties: Applications in Thermal Management and Energy Storage. *Appl. Sci.* **2014**, *4*, 525−547.
(45) Vasil'eva, N. A.; Uvarov, N. F. Electrical Conductivity of Magnesium Oxide as a Catalyst for Radical Chain Hydrocarbon Pyrolysis Reactions. *Kinet. Catal.* **2011**, *52*, 98−10.

DOI: 10.1021/acsami.5b03196
ACS Appl. Mater. Interfaces 2015, 7, 14397−14403